Tropical Journal of Pharmaceutical Research March 2023; 22 (3): 525-533
ISSN: 1596-5996 (print); 1596-9827 (electronic)

Available online at http://www.tjpr.org
http://dx.doi.org/10.4314/tjpr.v22i3.9

Original Research Article

Glabridin ameliorates DNFB-induced atopic dermatitis by suppressing MAPK/NF-κB signaling pathways in mice

Lu Cheng[1], Chuanqi Huang[1], Xin Xiong[1], Jie Jiang[1], Fuqian Wang[1], Dan Zhang[1], Shuting Liu[2], Yan Feng[3], Song Hu[1]*, Hong Zhang[1]

[1]Department of Pharmacy, [2]Department of Dermatology, [3]Department of Pathology, Wuhan No. 1 Hospital (Wuhan Hospital of Traditional and Western Medicine), Wuhan, China

For correspondence:* ***Email:* *huyaoshi@sina.com; dr_hong_zhang@163.com*

Sent for review: 14 June 2022 *Revised accepted: 27 February 2023*

Abstract

Purpose: *To investigate the anti-inflammatory mechanism of action of glabridin (GBD) isolated from glycyrrhizae radix et rhizoma (Glycyrrhiza glabra L.) using atopic dermatitis (AD) mouse model.*
Methods: *Nuclear factor-kappa B (NF-κB) and mitogen-activated protein kinase (MAPK) signaling pathways were investigated. The dorsal skin and serum of 2,4-dinitrofluorobenzene (DNFB)-induced AD mice were used to determine the levels of various inflammatory cytokines, including interferon (IFN)-γ, tumor necrosis factor (TNF)-α, interleukin (IL)-4, IL-5, IL-6, IL-13, and immunoglobulin E (IgE) by enzyme-linked immunosorbent assay (ELISA). The relative levels of inflammation-associated mRNA and signaling pathways were determined by real time-polymerase chain reaction (RT-PCR) and western blotting, respectively. Hematoxylin and eosin (H&E) staining was used to assess the effect of GBD on tissue thickening and inflammatory cell infiltration in mice with AD.*
Results: *Glabridin significantly relieved dorsal skin thickening, scabbing, and bleeding, and reduced the infiltration of inflammatory cells in mice with AD ($p < 0.05$). The levels of IFN-γ, TNF-α, IL-4, IL-5, IL-6, IL-13, and IgE were significantly reduced ($p < 0.05$ or 0.01). Moreover, the relative levels of IL-6 and IFN-γ mRNA showed a significant decrease ($p < 0.01$). Furthermore, GBD inhibited phosphorylation of MAPK signaling pathway and activation of NF-κB ($p < 0.05$ or 0.01).*
Conclusion: *Glabridin exerts an inhibitory effect on AD by blocking MAPK and NF-κB signaling pathways. This finding highlights the relationship between traditional Chinese medicine and modern AD therapeutic methods, which should be further investigated for its potential to be developed as an external anti-AD medicine.*

Keywords: *Glycyrrhizae radix et rhizome, Glycyrrhiza glabra, Atopic dermatitis, Traditional Chinese Medicine, Inflammation*

Tropical Journal of Pharmaceutical Research is indexed by Science Citation Index (SciSearch), Scopus, Web of Science, Chemical Abstracts, Embase, Index Copernicus, EBSCO, African Index Medicus, JournalSeek, Journal Citation Reports/Science Edition, Directory of Open Access Journals (DOAJ), African Journal Online, Bioline International, Open-J-Gate and Pharmacy Abstracts

INTRODUCTION

Atopic dermatitis (AD), also known as atopic eczema [1], is a refractory, chronic, allergic dermatosis, accompanied by intense pruritus and recurrent inflammatory symptoms [2] that affects 15 – 30 % of children and 2 – 10 % adults worldwide [3]. Owing to the diversiform genotype, multiple individual immunities, and various environmental stimuli [4], the treatment of AD is

challenging and it is difficult to obtain a satisfactory therapeutic outcome. Additionally, with an increase in age and aggravation of the disease, patients with allergies are more likely to develop allergic rhinitis and asthma, which considerably affect their physical and mental health.

The pathogenesis of AD is related to the overactive T-helper (Th)2 immune response and impaired barrier function of the skin. The excessive expression of activated Th2 cytokines such as interleukin (IL)-4, IL-5, IL-6, and IL-13 induces allergic reactions in the body and stimulates the synthesis of immunoglobulin E (IgE) by B cells, further aggravating the inflammatory response. Steroid hormones and immunosuppressants are the first-line treatment for AD owing to their potent anti-inflammatory and antipruritic effects. However, the long-term use of these drugs may cause serious side effects such as skin atrophy, and the topical use of these products on children's faces may cause topical telangiectasia. Therefore, many researchers have focused on the discovery of drugs from natural products as alternative therapies to improve the quality of life of patients with AD.

Glabridin (GBD, Figure 1) is derived from the extraction and processing of *Glycyrrhiza glabra*, and is mostly used in cosmetic formulae and the treatment of skin inflammation owing to its prominent antioxidant, anti-inflammatory, and melanin-inhibiting effect [5]. Although the role of GBD in dermatitis has often been demonstrated by its clinical efficacy, the molecular mechanism of its anti-AD effect is still lacking. Therefore, a mouse model of AD was used to determine the mechanism of GBD in alleviating AD.

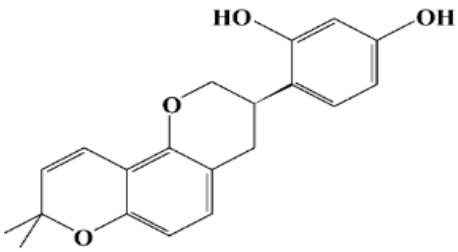

Figure 1: Chemical structure of glabridin

EXPERIMENTAL

Animals

Six-week-old female BALB/c mice (total of 48) were purchased from China Three Gorges University. Mice were fed in specific-pathogen-free conditions in the Experimental Animals Center of Huazhong University of Science and Technology and were maintained at a temperature of 20 - 22 ˚C and relative humidity of 55 %. They were subjected to a 12-h/12-h light/dark cycle and provided access to food and water *ad libitum*. The procedures for all experiments strictly complied with The Guidelines for the Care and Use of Laboratory Animals of the Institutional Animal Care and Use Committees of the United States (2011 Edition) [6]. The Animal Ethics Committee of Huazhong University of Science and Technology gave approval for the study (approval no. HUCMS202108006).

Establishment of a mouse model of AD, and treatment protocols

The AD model was established according to previous studies with appropriate modifications as shown in Figure 2. GBD (Shanghai R & D Center for Standardization of TCM, China), 2,4-dinitrofluorobenzene (DNFB, Sigma, USA), and dexamethasone (DEX, Huazhong Pharmaceutical Co., Ltd., China) were dissolved in dimethyl sulfoxide (DMSO, Dalian Meilum Biotechnology, China), organic solution (acetone : olive oil = 4 : 1), and saline, respectively. Mice were randomly and evenly divided into 6 groups (n = 8), and their dorsal hair was shaved with an electric shaver (Philips, Netherlands) and then the remaining hair was removed using a depilatory cream (Veet, France) on the first day. After 24 h, all mice except those in the normal control (NC) group were smeared with 50 µL 0.5 % DNFB on their dorsal side as the first stimulation. Subsequent stimulations were performed using 20 µL of 0.2 % DNFB on days 5, 8, 11, and 14. Mice in the NC group were smeared with DNFB-free solution (acetone : olive oil = 4 : 1) on the corresponding days indicated above. On days 6, 7, 9, 10, 12, 13, 15, and 16, DEX (5 mg/kg) was intraperitoneally injected as a positive control drug based on the body weights of mice (0.1 mL/10 g) in the DEX group [7]. Mice in the GBD-L, GBD-M and GBD-H groups (GBD-L: 50 mg/mL; GBD-M: 100 mg/mL; GBD-H: 200 mg/mL) were smeared with the corresponding GBD-DMSO solutions.

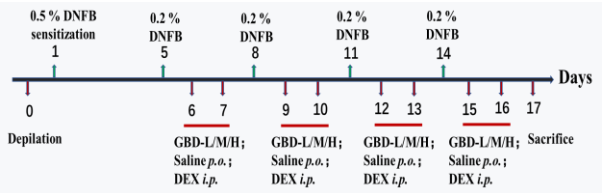

Figure 2: Schematic diagram of the drug-administration protocol in mice with AD

Evaluation of inflammation scores

Inflammation severity on the dorsal end of mice, including dryness, excoriation, hemorrhage, scaling, and scabbing, were physically evaluated by two researchers who did not participate in any other aspect of this experiment and assigned scores as follows: 0 (normal), 1 (mild inflammation), 2 (moderate inflammation), and 3 (severe inflammation) depending on the sizes of the inflammation.

Evaluation of serum cytokine levels

Mice were anesthetized with inhaled ether, and blood samples were obtained by cardiac puncture within 24 h after the last administration and quiescence overnight at 4 °C. The serum was collected by centrifugation (4 °C for 10 min at 1200 × *g*) and stored at -80 °C until subsequent experiments. Tumor necrosis factor (TNF)-α, interferon (IFN)-γ, IL-4, IL-5, IL-6, IL-13, and IgE contents in serum samples were quantified using the corresponding enzyme-linked immunosorbent assay (ELISA) kits (eBioscience, USA) according to manufacturer's instruction.

Quantitative real-time polymerase chain reaction (qRT-PCR)

Total RNA was collected using Trizol reagent (Invitrogen, USA), which was then synthesized into cDNA following the instructions of reverse transcriptional kit (Reverse Transcriptase M-MLV, Promega®, USA) and amplified using quantitative PCR (ABI PRISM® 7500 Sequence Detection System) with specific oligonucleotide primers (Sangon Biotech, China) of IL-6 or IFN-γ.

Table 1: Oligonucleotide primer sequences used in qRT-PCR

Gene	Primer	Sequence (5′-3′)
IFN-γ	Forward	CTCTGAGACAATGAACGCTACACACT
	Reverse	TGGCAGTAACAGCCAGAAACAG
IL-6	Forward	GATGCTACCAAACTGGATATAATC
	Reverse	GGTCCTTAGCCACTCCTTCTGTG
GAPDH	Forward	ACCACAGTCCATGCCATCAC
	Reverse	TCCACCACCCTGTTGCTGTA

The programmed temperature conditions were as follows: 2 min at 50 °C, 2 min at 95 °C, 95 °C for 15 s, and 60 °C for 32 s, repeated for 40 cycles. The relative amounts of IL-6 and IFN-γ mRNA were measured using fluorescence quantification kits (SYBR® Green, Invitrogen). The specific oligonucleotide primer sequences used are shown in Table 1.

Western blotting (WB)

Proteins were extracted from the dorsal skin of mice using RIPA kits (Pierce Biotechnology, USA), separated using sodium dodecyl sulfate-polyacrylamide gel electrophoresis (SDS-PAGE), then transferred to polyvinylidene difluoride (PVDF) membranes (0.45 mm, MILLIPORE, USA), and blocked in Tris-buffered saline of 5 % skim milk at 22 °C for 60 min. After being washed with Tris-buffer, the PVDF membranes were incubated with the corresponding primary antibodies (dilution ratio of 1 : 2000, Cell Signaling Technology, USA) overnight at 4 °C, the membranes were washed 3 times and incubated with secondary antibody for 1 h at 22 °C. The membranes were washed again 3 times with Tris-buffer containing 0.1 % (v/v) Tween® 20 and incubated for 2 min in chemiluminescence solution (MILLIPORE, USA). The grey intensity of bands was quantified by Gel Imaging System (Bio-Rad, CA) at the final step.

Histological examination

After sacrificing the mice, the dorsal skin was completely soaked in 10 % neutral formalin, fixed at 4 °C for 24 h, embedded with paraffin, and sectioned into 4 μm slices. The sections were dewaxed with xylene and gradient concentrations of ethanol, stained with hematoxylin and eosin (H & E), and transparentized with xylene for observation using an optical microscope (Olympus BX53, Japan) equipped with a digital camera (Olympus DP22, Japan).

Statistical analysis

Experimental data are expressed as mean ± standard error of the mean (SEM). Least significant difference (LSD) between groups was calculated using SPSS 20.0. $P < 0.05$ was considered statistically significant.

RESULTS

Severity of AD

The clinical features and dermatitis scores of DNFB-induced AD mice are shown in Figures 3 A and B, respectively. Signs of scabbing, epidermal thickening and bleeding caused by dry cracking were more conspicuous in mice in the DNFB group compared with those in the NC group. The epidermal injury was significantly

alleviated in mice in the GBD-M/H groups contrasted with those in the DNFB group (Figure 3 A). From days 4 to 16, the dermatitis scores were significantly elevated in DNFB mice contrasted with those in the NC group (Figure 3 B; $P < 0.01$), especially after day 7. From day 10 onward, the dermatitis scores in the GBD groups were significantly decreased versus the DNFB group mice ($p < 0.01$).

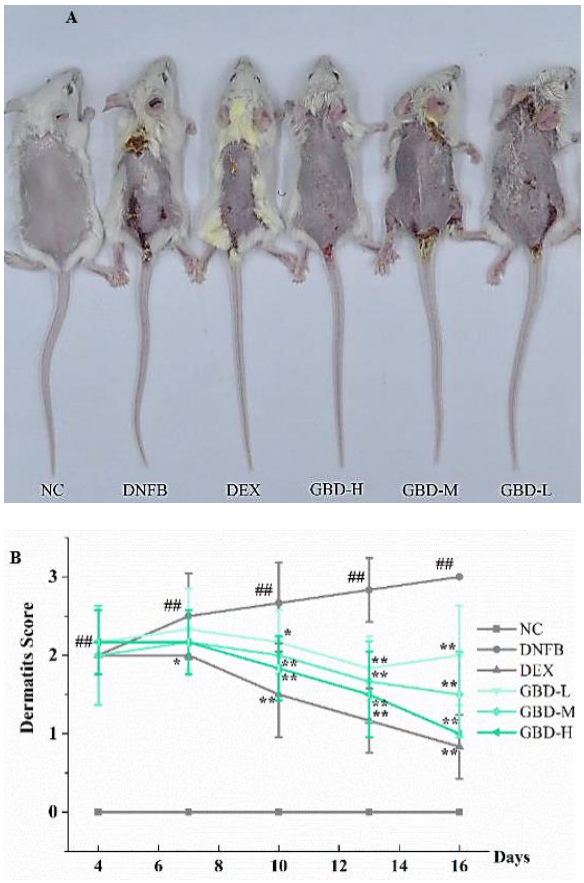

Figure 3: Anti-atopic dermatitis (AD) effect of glabridin (GBD) on DNFB-induced mice (n = 8). (A) Clinical symptoms of AD in representative mice in each group. (B) Dermatitis scores converted according to clinical symptoms of each group. Key: NC: normal control; DNFB: 2,4-dinitrofluorobenzene (DNFB)-induced mice; DEX: DNFB-induced and dexamethasone injected (5 mg/kg) mice; GBD-L: DNFB-sensitized mice + GBD-L (50 mg/mL); GBD-M: DNFB-induced mice + GBD-M (100 mg/mL); GBD-H: DNFB-sensitized mice + GBD-H (200 mg/mL). ##P < 0.01; *p < 0.05, **p < 0.01

Serum cytokines levels in mice with AD

Atopic dermatitis manifests as abnormal Th cytokine and IgE levels [8]. Cytokine and IgE levels in the DNFB group increased significantly compared with those in the NC group (Figure 4; $p < 0.01$), whereas GBD intervention significantly inhibited IL-4, IL-5, IL-6, IL-13, IFN-γ, TNF-α, and IgE production in a dose-dependent manner ($p < 0.01$).

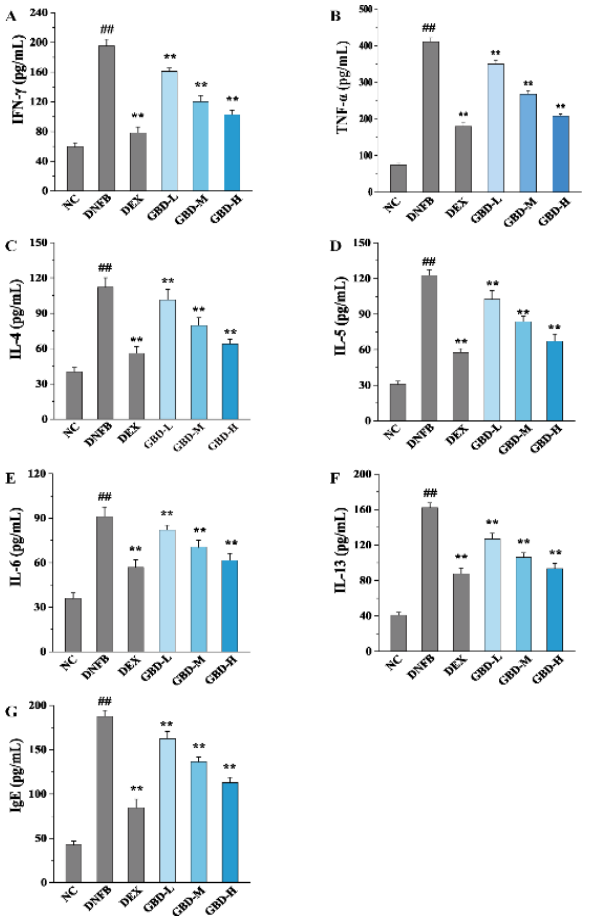

Figure 4: Effects of glabridin (GBD) on IFN-γ (A), TNF-α (B), IL-4 (C), IL-5 (D), IL-6 (E), IL-13 (F), and IgE (G) levels in the skins of mice with AD ($n = 8$). **Key:** NC: normal control; DNFB: DNFB-sensitized mice; DEX: DNFB-sensitized mice + dexamethasone injection (5 mg/kg); GBD-L: DNFB-sensitized mice + GBD-L (50 mg/mL); GBD-M: DNFB-sensitized mice + GBD-M (100 mg/mL); GBD-H: DNFB-sensitized mice + GBD-H (200 mg/mL). ##Significant difference from NC, $P < 0.01$, *$p < 0.05$ and **$p < 0.01$ versus the DNFB group

Relative contents of IFN-γ and IL-6 mRNA

Changes in mRNA levels of specific inflammatory cytokines serve as indicators of the inflammatory response [9]. The IL-6 and IFN-γ, which are considered the key cytokines in AD genesis, are selected to study the effects of GBD in AD. Quantitative real-time PCR results are reported in Figure 5. The relative contents of IL-6 and IFN-γ mRNA in the DNFB group were significantly higher compared with those in the NC group ($p < 0.01$), whereas the levels in the GBD-L, GBD-M, and GBD-H groups were significantly decreased compared with those in the DNFB group ($p < 0.01$). The mRNA levels of IL-6 in the GBD-M and GBD-H groups decreased significantly compared with those in the DNFB group ($p < 0.01$).

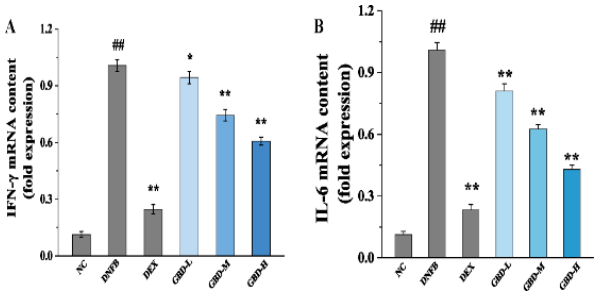

Figure 5: Effects of glabridin (GBD) on the mRNA expression of IFN-γ (A) and IL-6 (B); (n = 8). ***Key:*** NC: normal control; DNFB: 2,4-dinitrofluorobenzene (DNFB)-induced mice; DEX: DNFB-induced and dexamethasone injected (5 mg/kg) mice; GBD-L: DNFB-sensitized mice + GBD-L (50 mg/mL); GBD-M: DNFB-induced mice + GBD-M (100 mg/mL); GBD-H: DNFB-sensitized mice + GBD-H (200 mg/mL). $^{\#\#}P < 0.01$; *$p < 0.05$, **$p < 0.01$

Effect of GBD on mitogen-activated protein kinase (MAPK) and NF-κB signaling pathways

Mitogen-activated protein kinase (MAPK) signaling pathway consists of the extracellular regulated kinase (ERK), c-jun N-terminal kinase (JNK), and p38 MAPK, and plays a role in regulating and stimulating the inflammatory response. NF-κB on the other hand plays a role in the inflammatory response and is involved in the pathogenesis of AD [10]. Western blot result revealed that IκB-α and cytoplasmic NF-κB p65 were positively correlated with the dose of GBD, whereas p-p38 MAPK, p38 MAPK, p-ERK1/2, ERK1/2, p-JNK, JNK, total NF-κB p65, p-IκB-α, and nuclear NF-κB p65 were negatively correlated with the dose of GBD (Figure 6).

The gray-scale values showed that MAPK expression in DNFB group was significantly increased versus that in NC group ($p < 0.01$). The GBD not only suppressed p38 MAPK, JNK, and ERK production but also inhibited p38 MAPK, JNK, and ERK phosphorylation compared with DNFB group ($p < 0.01$) (Figure 7 A, B, and C).

Besides, the gray-scale values of total (Figure 7 D) and nuclear (Figure 7 F) NF-κB p65, and p-IκB-α (Figure 7 H) in DNFB group increased significantly, whereas cytoplasmic NF-κB p65 (Figure 7 E) and IκB-α (Figure 7 G) levels were reduced compared with that in the NC group ($p < 0.01$). The GBD-treated groups showed a remarkable downregulation of total (Figure 7 D) and nuclear (Figure 7 F) NF-κB p65, along with the p-IκB-α (Figure 7 H) compared with the DNFB group ($p < 0.01$), whereas upregulation of cytoplasmic NF-κB p65 (Figure 7 E) and IκB-α (Figure 7 G) was noted in the GBD-treated groups compared with that in the DNFB group ($p < 0.01$).

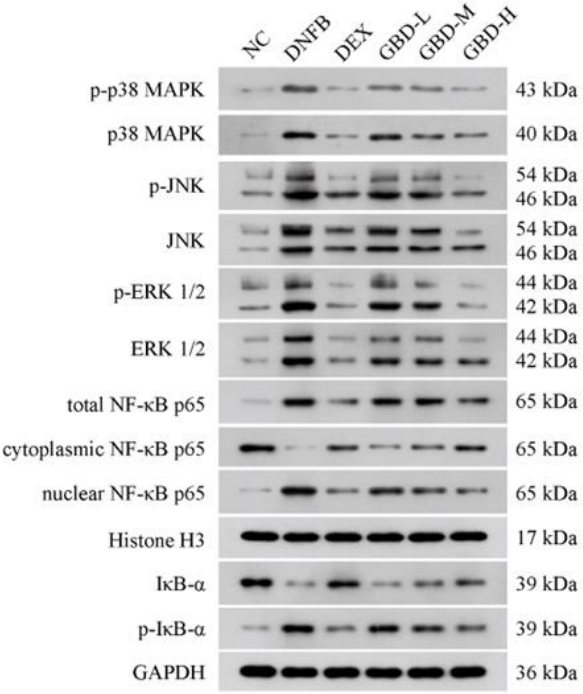

Figure 6: Effects of glabridin (GBD) on MAPK and NF-κB using WB ($n = 3$). Relevant protein bands showing phosphorylated p38 MAPK/p38 MAPK

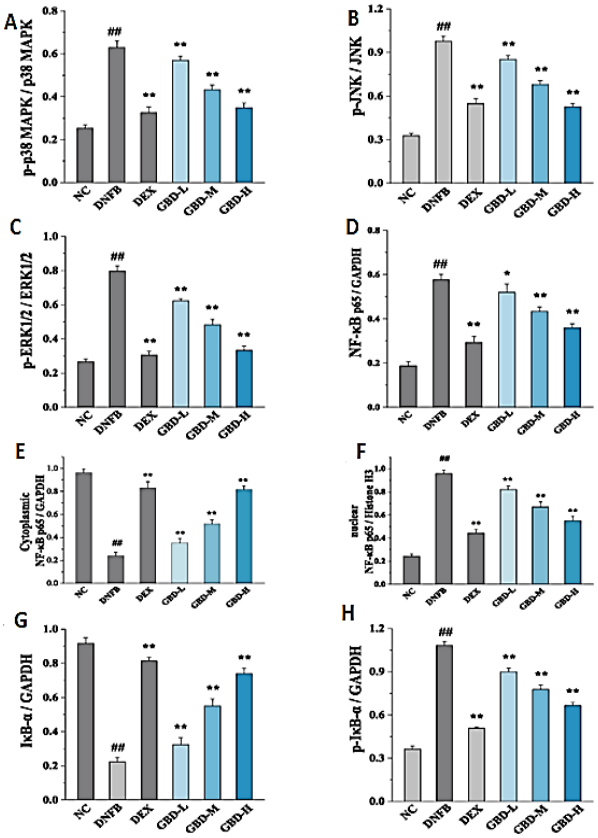

Figure 7: Effects of glabridin (GBD) on MAPK and NF-κB using WB ($n = 8$). Relevant protein bands (A), Phosphorylated JNK/JNK (B), phosphorylated ERK/

ERK (C), total NF-κB p65 (D), cytoplasmic NF-κB p65 (E), nuclear NF-κB p65 (F), IκB-α (G), and p-IκB-α (H). **Key:** NC: normal control; DNFB: 2,4-dinitrofluorobenzene (DNFB)-induced mice; DEX: DNFB-induced and dexamethasone injected (5 mg/kg) mice; GBD-L: DNFB-sensitized mice + GBD-L (50 mg/mL); GBD-M: DNFB-induced mice + GBD-M (100 mg/mL); GBD-H: DNFB-sensitized mice + GBD-H (200 mg/mL). $^{\#\#}P < 0.01$, $*p < 0.05$, $**p < 0.01$

Histopathological characteristics of the dorsal skin of mice with AD

Hematoxylin and Eosin staining was performed on the dorsal skin of mice with AD. As shown in Figure 8, the epidermal tissue of mice from the DNFB group showed exfoliation, dehiscing, and significant thickening, and numerous inflammatory cells were observed compared with mice in the NC group. The thickness of, and damage to epidermal tissue obtained from mice in the GBD groups were ameliorated (Figure 9), and the abundance of inflammatory cells was suppressed compared with that in DNFB group

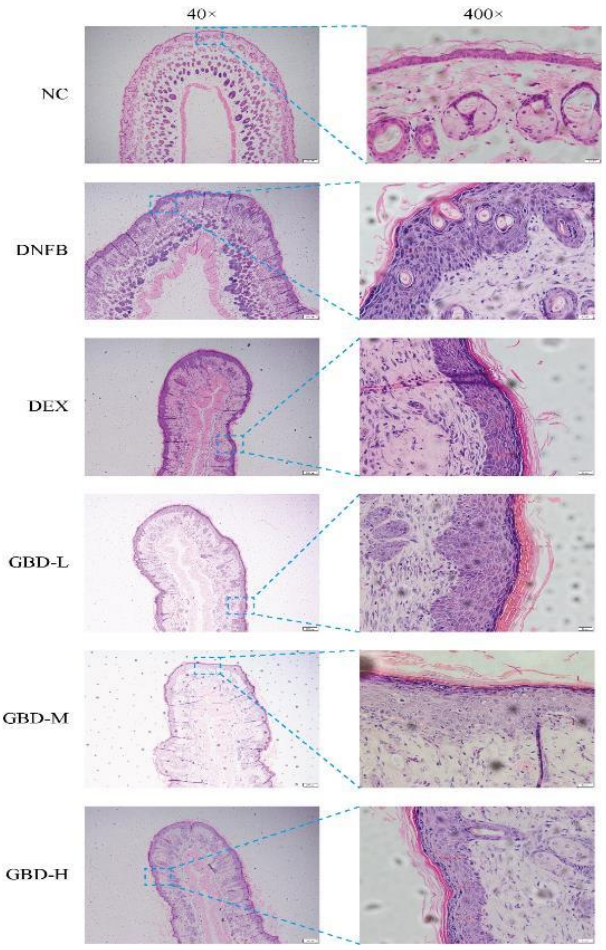

Figure 8: Effects of glabridin (GBD) on inflammatory cell infiltration showing dorsal skin of mice with AD dissected for H&E staining

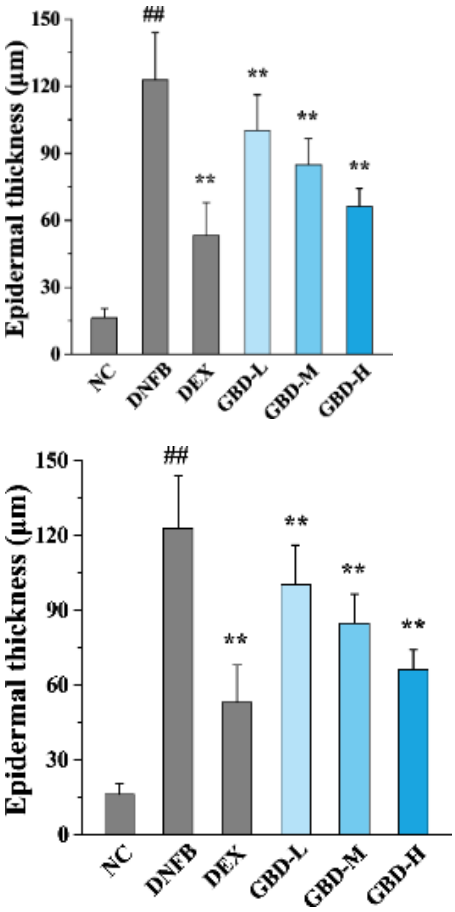

Figure 9: Effects of glabridin (GBD) on inflammatory cell infiltration showing epidermal thickness of infiltrating cells calculated for each group (n = 8). ***Key:*** NC: normal control; DNFB: 2,4-dinitrofluorobenzene (DNFB)-induced mice; DEX: DNFB-induced and dexamethasone injected (5 mg/kg) mice; GBD-L: DNFB-sensitized mice + GBD-L (50 mg/mL); GBD-M: DNFB-induced mice + GBD-M (100 mg/mL); GBD-H: DNFB-sensitized mice + GBD-H (200 mg/mL). $^{\#\#}P < 0.01$; $*p < 0.05$, $**p < 0.01$

DISCUSSION

Atopic dermatitis which usually occurs in children is a cutaneous inflammatory condition associated with inherited characteristics [11]. With the worsening of AD, the patient's skin becomes more sensitive and is likely to cause epidermal damage, such as papules, erythema, and pigmentation. Furthermore, AD usually results in inferiority complex, anxiety, and a lack of confidence among children, leading to sleep disorders and other negative impacts on their lives. Immunosuppressants and topical steroids are currently the main therapeutic options to treat AD. However, the long-term use of these drugs may cause side effects such as skin thinning, vasoconstriction, and liver and kidney toxicity. Therefore, there is a need to discover alternative therapies for AD management to improve patient compliance and quality of life [12]. As a unique

active component of G. glabra L [13], GBD has been widely used in various premium cosmetics and anti-dermatitis drugs owing to its excellent skin care properties and whitening effects though its potential anti-inflammatory mechanism is not known. Therefore, in this study, the underlying mechanism of GBD that is responsible for its anti-AD effect has been investigated.

The excessive secretion of Th2 cytokines leads to infiltration and deposition of eosinophils, mast cells, and other immune cells, whereas histamine release can cause skin itching, dryness, bleeding, scabbing, and epidermal thickening in AD. Although the epidermal symptoms in mice with AD were conspicuous in the DNFB group, skin damage in mice in the GBD groups was significantly ameliorated, especially in those in GBD-H group, and the effect was almost similar to that of mice in DEX group. Dermatitis scores further confirmed that GBD could alleviate epidermal tissue symptoms with DNFB treatment, including thickening, bleeding, and cracking. Furthermore, microscopy findings after H & E staining supported that epidermal thickening was suppressed in the GBD groups, particularly in the GBD-H and DEX groups ($p < 0.01$), indicating that GBD significantly ameliorated the symptoms of AD compared with the apparent symptoms and microscopic pathology.

The trigger of deterioration in AD is accompanied by abnormal secretion of Th1, Th2, and Th17 cytokines. During the process of AD, more Th cells develop as Th2 cells and combine with mast cells, eosinophils, and basophils to secrete IL-4, IL-5, IL-6, and IL-13 [14]. Interleukin-4 and IL-13 promote the synthesis of IgE and IL-5, which are the markers of AD in serum [15] and the key activator of the chemokine eotaxin, respectively. Besides, IL-5 is responsible for the infiltration of eosinophils, while excessive eosinophils lead to increased IgE secretion. ELISA revealed that GBD significantly inhibited IL-4, IL-5, IL-13, and IgE; therefore, GBD could inhibit the generation and development of AD.

The IFN-γ and TNF-α are Th1 cytokines. IFN-γ inhibits IgE synthesis by suppressing B cells, whereas TNF-α is one of the main pro-inflammatory factors in AD associated with IL-6 release. The induced secretion of excessive IL-6 leads to the synthesis of inflammatory proteins in the acute phase, which interferes with skin barrier function and activates the MAPK signaling pathway [16]. In this study, IFN-γ, TNF-α, and IL-6 were comprehensively inhibited, indicating that GBD had a significant effect on AD.

Besides, GBD significantly suppressed IL-6 and IFN-γ mRNA levels in the dorsal skin of AD mice. This function trend was parallel to the results from serum ELISA. A comprehensive analysis of ELISA and qPCR findings showed that the inflammatory factors related to AD were effectively inhibited by GBD, indicating the therapeutic effect of GBD in AD.

The MAPK and NF-κB signaling pathways are activated in successive inflammatory responses and are especially related to the trigger and development of AD [17]. As a pivotal signaling pathway, MAPK not only activates NF-κB but also promotes the transformation and secretion of inflammatory cytokines such as TNF-α and IL-6. In this study, GBD inhibited p38 MAPK, JNK, and ERK phosphorylation in a dose-dependent manner in the GBD groups compared with the DNFB group ($p < 0.01$). Particularly, mice in the GBD-H group exhibited anti-inflammatory effects comparable with those in the DEX group ($p > 0.05$). These findings indicated that GBD could effectively suppress the activation of MAPK signaling pathway to ameliorate AD.

NF-κB is a nuclear transcription factor involved in the secretion of cytokines when inflammation occurs [18]. Under normal circumstances, IκB binds to the NF-κB dimer in the cytoplasm. When histamine, antigens, or inflammatory cytokines stimulate cells, the phosphorylated IκB is recognized by lysosomes and degraded. The NF-κB dimer that is released enters the nucleus to bind relevant DNA and transcribes a string of inflammatory cytokines. It was observed that p-IκB-α was significantly decreased and cytoplasmic NF-κB p65 was significantly elevated in mice in the GBD groups compared with DNFB group ($p < 0.01$), indicating that the phosphorylation and ubiquitination of IκBα in the cytoplasm were inhibited. This process inhibits the cleavage of IκB-α and the entry of NF-κB dimer into the nucleus, thus blocking NF-κB activation. The reduction of nuclear NF-κB p65 in the GBD groups was comparable with DNFB group ($p < 0.01$). Further confirming that GBD effectively suppressed the activation of NF-κB signaling pathway in a dose-dependent manner

CONCLUSION

Glabridin inhibits the phosphorylation of p38 MAPK, JNK, and ERK, indicating that it could inhibit the activation of MAPK signaling pathway and block the progression of AD. Moreover, activation of NF-κB and the inflammatory reaction chain in the nucleus is inhibited by GBD. These findings show that GBD could exert an inhibitory effect on AD by blocking MAPK and

NF-κB signaling pathways. Thus, there a likely link between traditional Chinese medicine and modern AD therapeutic methods, that requires further investigation.

DECLARATIONS

Acknowledgements

This research was funded by the Scientific Research Foundation for Young Scientist of Wuhan No. 1 Hospital (grant no. 2020Q02).

Funding

None provided.

Ethical approval

None provided.

Availability of data and materials

The datasets used and/or analyzed during the current study are available from the corresponding author on reasonable request.

Conflict of Interest

No conflict of interest associated with this work.

Contribution of Authors

We declare that this work was performed by the authors named in this article and all liabilities pertaining to the claims related to the content of this article will be borne by the authors. Hong Zhang and Song Hu designed the manuscript; Xin Xiong, Chuanqi Huang, Lu Cheng, Jie Jiang, Fuqian Wang, Dan Zhang, Shuting Liu, and Yan Feng performed the experiments and analyzed the data. All authors read and approved the final manuscript. Lu Cheng and Chuanqi Huang contributed equally to this work.

REFERENCES

1. *Park G, Lee SH, Oh DS, Kim YU. Melatonin inhibits neuronal dysfunction associated with neuroinflammation by atopic psychological stress in NC/Nga atopic-like mouse models. J Pineal Res 2017; 63(2): e12420.*
2. *Lee J-H, Lim J-Y, Jo E H, Noh H M, Park S, Park M C, Kim D-K. Chijabyukpi-Tang inhibits pro-inflammatory cytokines and chemokines via the Nrf2/HO-1 signaling pathway in TNF-α/IFN-γ-stimulated HaCaT cells and ameliorates 2,4-dinitrochlorobenzene-induced atopic dermatitis-like skin lesions in mice. Front Pharmacol 2020; 11: 1018.*
3. *Cho K, Kang MC, Parveen A, Yumnam S, Kim SY. Anti-inflammatory effect of chloroform fraction of Pyrus ussuriensis Maxim. Leaf extract on 2, 4-dinitrochlorobenzene-induced atopic dermatitis in NC/NGA mice. Nutrients 2019; 11(276): 2-12.*
4. *Sung YY, Kim SH, Yang WK, Park YC, Kim HK. Bleomycin aggravates atopic dermatitis via lung inflammation in 2,4-dinitrochlorobenzene-induced NC/NGA mice. Front Pharmacol 2018; 9: 578.*
5. *Wahab S, Annadurai S, Abullais SS, Das G, Ahmad W, Ahmad MF, Kandasamy G, Vasudevan R, Ali MS, Amir M. Glycyrrhiza glabra (Licorice): A comprehensive review on its phytochemistry, biological activities, clinical evidence, and toxicology. Plants 2021; 10(12): 137:111393. doi: 10.1016/j.biopha.2021.111393*
6. *Guide for the Care and Use of Laboratory Animals. 2011. Washington (DC).*
7. *Cha KJ, Im MA, Gu A, Kim DH, Lee D, Lee JS, Lee JS, Kim IS. Inhibitory effect of Patrinia scabiosifolia link on the development of atopic dermatitis-like lesions in human keratinocytes and NC/NGA mice. J Ethnopharmacol 2017; 206: 135-143.*
8. *Yang JH, Do HJ, Lee E, Yim NH, Cho WK, Park KI, Ma JY. Jageum-Jung improves 2,4-dinitrochlorobenzene-induced atopic dermatitis-like skin lesions in mice and suppresses pro-inflammatory chemokine production by inhibiting TNF-α/IFN-γ-induced STAT-1 and NFκB signaling in HaCaT cells. J Ethnopharmacol 2018; 221: 48-55.*
9. *Ham B, Kim M, Son YJ, Chang S, Jung SH, Nho CW, Kwon MJ. Inhibitory effects of Pterocarpus santalinus extract against IgE/antigen-sensitized mast cells and atopic dermatitis-like skin lesions. Planta Med 2019; 85(7): 599-607.*
10. *Clarysse K, Pfaff CM, Marquardt Y, Huth L, Kortekaas KI, Kluwig D, Luscher B, Gutermuth J, Baron J. JAK1/3 inhibition preserves epidermal morphology in full-thickness 3D skin models of atopic dermatitis and psoriasis. J Eur Acad Dermatol Venereol 2019; 33(2): 367-375.*
11. *Parisi JDS, Correa MP, Gil CD. Lack of endogenous Annexin A1 increases mast cell activation and exacerbates experimental atopic dermatitis. Cells 2019; 8(1): 2-10.*

12. Sae-Wong C, Mizutani N, Kangsanant S, Yoshino S. Topical skin treatment with Fab fragments of an allergen-specific IgG1 monoclonal antibody suppresses allergen-induced atopic dermatitis-like skin lesions in mice. Eur J Pharmacol 2016; 779: 131-137.
13. Parlar A, Arslan SO, Cam SA. Glabridin alleviates inflammation and nociception in rodents by activating BKCA channels and reducing NO levels. Biol Pharm Bull 2020, 43(5): 884-897.
14. Hong SH, Ku JM, Kim HI, Kim TY, Seo HS, Shin YC, Ko SG. Topical application of KAJD attenuates 2,4-dinitrochlorobenzene-induced atopic dermatitis symptoms through regulation of IgE and MAPK pathways in BALB/C mice and several immune cell types. Front Pharmacol 2019; 10: 1097.
15. Park KI, Kim DG, Yoo JM, Ma JY. The herbal medicine KIOM-MA128 inhibits the antigen/IgE-mediated allergic response in vitro and in vivo. Molecules 2016; 21(8): 2-11.
16. Lee HJ, Kim MH, Choi YY, Kim EH, Hong J, Kim K, Yang WM. Improvement of atopic dermatitis with topical application of Spirodela polyrhiza. J Ethnopharmacol 2016, 180: 12-17.
17. Choo GS, Lim DP, Kim SM, Yoo ES, Kim SH, Kim CH, Woo JS, Kim HJ, Jung JY. Antiinflammatory effects of Dendropanax morbifera in lipopolysaccharide-stimulated RAW264.7 macrophages and in an animal model of atopic dermatitis. Mol Med Rep 2019; 19(3): 2087-2096.
18. Cai B, Seong KJ, Bae SW, Chun C, Kim WJ, Jung JY. A synthetic diosgenin primary amine derivative attenuates LPS-stimulated inflammation via inhibition of NF-kappaB and JNK MAPK signaling in microglial BV2 cells. J Int Immunopharmacol 2018; 61: 204-214.